

*Climate of the Past Discussions* is the access reviewed discussion forum of *Climate of the Past*

# Climate and CO<sub>2</sub> modulate the C<sub>3</sub>-C<sub>4</sub> balance and $\delta^{13}\text{C}$ signal in simulated vegetation

O. Flores<sup>1</sup>, E. S. Gritti<sup>1,2</sup>, and D. Jolly<sup>2</sup>

<sup>1</sup>CEFE, UMR 5175 CNRS, 1919, route de Mende, 34293, Montpellier cedex 5, France

<sup>2</sup>ISEM, UMR 5554 CNRS/Univ. Montpellier II, Case 61, 34095 Montpellier cedex 5, France

Received: 25 February 2009 – Accepted: 2 March 2009 – Published: 31 March 2009

Correspondence to: O. Flores (olivier.flores@cefe.cnrs.fr)

Published by Copernicus Publications on behalf of the European Geosciences Union.

CPD

5, 1187–1213, 2009

C<sub>3</sub>-C<sub>4</sub> balance and  
 $\delta^{13}\text{C}$  in simulated  
vegetation

O. Flores et al.

Title Page

Abstract

Introduction

Conclusions

References

Tables

Figures

⏪

⏩

◀

▶

Back

Close

Full Screen / Esc

Printer-friendly Version

Interactive Discussion



## Abstract

Fossil pollen data and  $\delta^{13}\text{C}$  measurements from cores collected in peatbogs or lakes have shown major changes in the terrestrial vegetation during Late Quaternary. Although the effect of climate on the  $\text{C}_3\text{-C}_4$  balance has been discussed for 50 years, the impact of a low atmospheric  $\text{CO}_2$  during the Last Glacial Maximum (LGM) was emphasized recently and conflicting evidence exists. In this paper, we use a physiologically-based biome model (BIOME4) in an iterative mode to simulate vegetation response to changing mean climate conditions and atmospheric  $\text{CO}_2$  partial pressure ( $p_{\text{CO}_2}$ ). In particular, we investigate the transition from LGM to present conditions in two sites which changed from either a  $\text{C}_4$ - or a  $\text{C}_3$ -dominated vegetation to the opposite pole, respectively at Kuruyange (Burundi) and Lingtaï (Central Loess Plateau, China). The response of the  $\text{C}_3\text{-C}_4$  balance and  $\delta^{13}\text{C}$  signal in the simulated vegetation are investigated. The results show that the vegetation is primarily sensitive to temperature and  $p_{\text{CO}_2}$ . Rainfall impacted the simulated variables below a threshold which decreased with higher  $p_{\text{CO}_2}$ . Climate and  $p_{\text{CO}_2}$  interacted differently between the two sites showing indirect effects on the  $\delta^{13}\text{C}$  signal. Moreover, the plant functional types (PFTs) differed in their composition and in their response between the two sites, emphasizing that the competition between  $\text{C}_3$  and  $\text{C}_4$  plants cannot be hardly considered as a simple binary scheme. Our results confirm the advantages of using process-based models to understand past vegetation changes and the need to take account of multiple drivers when the  $\text{C}_3\text{-C}_4$  balance is reconstructed from a palaeo- $\delta^{13}\text{C}$  signal.

## 1 Introduction

Evidence of the relative influence of climate and  $p_{\text{CO}_2}$  on the balance between  $\text{C}_3$  and  $\text{C}_4$  plants come from two sources essentially. The first type of evidence derives from current patterns which indicate that  $\text{C}_4$  plants abound more in warm and dry conditions. Meanwhile, meta-analysis and experiments in controlled conditions have

CPD

5, 1187–1213, 2009

## $\text{C}_3\text{-C}_4$ balance and $\delta^{13}\text{C}$ in simulated vegetation

O. Flores et al.

Title Page

Abstract

Introduction

Conclusions

References

Tables

Figures

⏪

⏩

◀

▶

Back

Close

Full Screen / Esc

Printer-friendly Version

Interactive Discussion



**C<sub>3</sub>-C<sub>4</sub> balance and  
 $\delta^{13}\text{C}$  in simulated  
vegetation**

O. Flores et al.

Title Page

Abstract

Introduction

Conclusions

References

Tables

Figures

◀

▶

◀

▶

Back

Close

Full Screen / Esc

Printer-friendly Version

Interactive Discussion



led to mixed results with respect to the competitive advantage of C<sub>4</sub> species at low CO<sub>2</sub> concentration (Wand et al., 1999; Ward et al., 1999,  $p_{\text{CO}_2}$ ). C<sub>4</sub> species are less sensible to photorespiration than C<sub>3</sub> plants (Sage, 2004) and can tolerate low  $p_{\text{CO}_2}$ . The second type of evidence derives from the analysis of  $\delta^{13}\text{C}$  signal along cores. Because they discriminate <sup>13</sup>C differently during photosynthesis, C<sub>3</sub> and C<sub>4</sub> species have different carbon isotopic composition ( $\delta^{13}\text{C}$ ), and hence leave different isotopic signal in paleorecords. Sequences of  $\delta^{13}\text{C}$  sampled along cores are routinely used to the reconstruct C<sub>3</sub>-C<sub>4</sub> balance, i.e. the proportion of C<sub>4</sub> for instance in the vegetation (Gu et al., 2003; Wang et al., 2008) which we note  $r_{\text{C}_4}$ . Meanwhile, pollen assemblages can be used to reconstruct climatic parameters and  $p_{\text{CO}_2}$  and their changes through time (Guiot, 1994; Guiot et al., 2000).

Different patterns of  $\delta^{13}\text{C}$  during the transition from the Last Glacial Maximum (LGM) to Holocene led to various conclusions regarding the relative influence of climate and CO<sub>2</sub> on the C<sub>3</sub>-C<sub>4</sub> balance (Aucour et al., 1999; Huang et al., 2001; Gu et al., 2003). Large changes occurred in climatic conditions and in the chemical composition of the atmosphere. The concentration of atmospheric CO<sub>2</sub> gradually increased from 180 ppmv to 270 ppmv, which alone could induce vegetation changes (Cole and Monger, 1994; Jolly and Haxeltine, 1997; Street-Perrott et al., 1997). Samples from the intertropical African highlands revealed high values of  $\delta^{13}\text{C}$  during the LGM ( $> -18\%$ ), and low during the late Holocene (Aucour and Hillaire-Marcel, 1994; Aucour et al., 1999,  $-28.5 < \delta^{13}\text{C} < -19.5\%$ ). These variations were consistent with pollen records taken in peatbogs or lakes which revealed a shift in the C<sub>3</sub>-C<sub>4</sub> balance at the end of the LGM, from grasslands with C<sub>4</sub> species to montane forests with a majority of C<sub>3</sub> trees (Jolly et al., 1997).

Accumulated evidence moderated this view and several studies concluded that climate was the main control on the abundance of C<sub>4</sub> plants (Huang et al., 2001; Gu et al., 2003; Zhang et al., 2003; Liu et al., 2005a). The comparison of  $\delta^{13}\text{C}$  sequences in lakes of South America revealed opposed trends (Huang et al., 2001). The authors concluded that differing trajectories originated from differing local climatic conditions,

## C<sub>3</sub>-C<sub>4</sub> balance and $\delta^{13}\text{C}$ in simulated vegetation

O. Flores et al.

Title Page

Abstract

Introduction

Conclusions

References

Tables

Figures

◀

▶

◀

▶

Back

Close

Full Screen / Esc

Printer-friendly Version

Interactive Discussion



since all sites shared the same  $p_{\text{CO}_2}$  (Huang et al., 2001). At a regional/continental scale, aridity appeared as the dominant control on the C<sub>3</sub>-C<sub>4</sub> balance (Schefus et al., 2003). Reported  $\delta^{13}\text{C}$  sequences from central China reveal lower values during the LGM than during late Holocene (Gu et al., 2003; Wang et al., 2008). This trend was interpreted as an increase of the abundance of C<sub>4</sub> species in time in response to warmer conditions (Zhang et al., 2003) or increased monsoon intensity with higher temperature and rainfall (Liu et al., 2005a).

The reconstruction of the C<sub>3</sub>-C<sub>4</sub> balance in empirical studies is based on a linear model between the  $\delta^{13}\text{C}$  and  $r_{\text{C}_4}$  (e.g. Gu et al., 2003):  $\delta^{13}\text{C} = r_{\text{C}_4} \times \delta^{13}\text{C}_{\text{C}_4} + (1 - r_{\text{C}_4}) \times \delta^{13}\text{C}_{\text{C}_3}$  where  $\delta^{13}\text{C}_{\text{C}_4}$ , and  $\delta^{13}\text{C}_{\text{C}_3}$  are the values of  $\delta^{13}\text{C}$  of the C<sub>3</sub> and C<sub>4</sub> poles, the most commonly used values being  $-26$  and  $-13\text{‰}$  (Deines, 1980), respectively. However, climate and  $p_{\text{CO}_2}$  have direct effects on  $r_{\text{C}_4}$  and on  $\delta^{13}\text{C}_{\text{C}_3}$  and  $\delta^{13}\text{C}_{\text{C}_4}$  as well (Wang et al., 2008). The carbon isotopic ratio of C<sub>3</sub> plants increases with decreasing water availability for instance. This trend has been evidenced along rainfall gradient (Liu et al., 2005b; Wang et al., 2008). In C<sub>4</sub> plants, the response of  $\delta^{13}\text{C}$  to water stress depends on the degree of leakiness. C<sub>4</sub> plants tolerate low ratio of intercellular to atmospheric  $p_{\text{CO}_2}$  ratio ( $\frac{c_i}{c_a}$ ) during warm hours, whereas stomatal conductance of C<sub>3</sub> strongly decreases under water stress.

The purpose of this work is to simulate the C<sub>3</sub>-C<sub>4</sub> balance in various conditions of climate and atmospheric CO<sub>2</sub> to investigate their respective influence. We use a process-based equilibrium model to simulate the Net Primary Production of the vegetation as well as the respective values of  $\delta^{13}\text{C}$  in C<sub>3</sub> and C<sub>4</sub> in designed climatic scenarii. We use the model outputs to study the relationships between climate and  $p_{\text{CO}_2}$  and two features of the simulated vegetation that are the proportion of C<sub>4</sub> NPP (C<sub>3</sub>-C<sub>4</sub>) and the carbon isotope composition of the bulk vegetation ( $\delta^{13}\text{C}$ ). Namely, we consider two sets of climatic conditions and  $p_{\text{CO}_2}$  that correspond to the current climate and to LGM conditions and investigate the responses to the two types of forcings in two contrasted sites located in the highlands of equatorial Africa and on the central Loess plateau in

China.

## 2 Methods

### 2.1 Site selection

We chose to focus on sites differing in current and past climatic conditions and vegetation in addition of being located in areas where reconstructions of paleoclimate have been previously conducted. Two sites were selected for comparison, one located in intertropical Africa (Kuruyange) and one located on the loess plateau in China (Lingtaï).

Kuruyange lies in the interlacustrine highlands in Central Africa (Burundi) in the current altitudinal range of montane forests. These forests are present in the area as fragments of broad-leaved forest inbetween cultivated and grazed land (Jolly et al., 1997). In Kuruyange as in intertropical Africa overall, the local vegetation was essentially composed of cold grasses and scrub during the LGM (Hamilton, 1982; Bonnefille and Riollet, 1988; Vincens, 1991; Taylor, 1992; Jolly and Haxeltine, 1997). After ca. 10–11 kyr BP, it was progressively replaced by a tropical montane forest (Coetzee, 1967; Hamilton, 1972; Taylor, 1990, 1993; Bonnefille et al., 1991, 1995; Vincens, 1991; Jolly et al., 1994). In pollen records, Poaceae and Cyperaceae, including C<sub>4</sub> species, are abundant at the LGM. After 10 kyr BP, the grasses tend to disappear from records, whereas C<sub>3</sub> trees become more abundant.

Lingtaï lies on the Loess plateau in central China. The vegetation in the area is a mixed forest of temperate coniferous and broad-leaved trees and many grass species. Studies of  $\delta^{13}\text{C}$  in core sequences showed that C<sub>4</sub> plants were absent of the vegetation at the LGM which was mostly steppe and desert vegetation (Yu et al., 2000). During the Holocene, C<sub>4</sub> plants became more abundant (Gu et al., 2003; Wang et al., 2008).

CPD

5, 1187–1213, 2009

## C<sub>3</sub>-C<sub>4</sub> balance and $\delta^{13}\text{C}$ in simulated vegetation

O. Flores et al.

Title Page

Abstract

Introduction

Conclusions

References

Tables

Figures

⏪

⏩

◀

▶

Back

Close

Full Screen / Esc

Printer-friendly Version

Interactive Discussion



## 2.2 Current and past climate

Climatic data were extracted from the  $10 \times 10'$  grids published by New et al. (2002) considering the nearest grid point from sites location. Monthly precipitations in mm/month, mean temperatures in  $^{\circ}\text{C}$ , and mean sunshine in % of day length were taken at  
5 (–3.583°, 29.750°, 1850 m a.s.l.) for Kuruyange in Burundi, and (35.083°, 107.583°, 1180 m a.s.l.) for Lingtaï in China.

Annual precipitation and mean annual temperature were respectively 1370 mm, 18.0°C for Kuruyange, and 600 mm, 10.2°C for Lingtaï. Kuruyange has a typical equatorial climate with consistent monthly temperatures throughout the year, three warm  
10 and dry months during summer and high rainfall from September to May (Fig. 1). Climatic parameters were estimated respectively about  $4 \pm 2^{\circ}\text{C}$  and  $40 \pm 10\%$  lower at the LGM in the area (Bonnefille et al., 1990; Bonnefille and Chalié, 2000).

Lingtaï has a continental climate with a cold and dry winter and low rainfall concentrated in summer. The climate on the Loess plateau is largely controlled by the East  
15 Asian Monsoon (EAM) system (Balsam et al., 2004). Estimates of mean annual temperature anomaly at the LGM range between  $-7$  and  $-10^{\circ}\text{C}$  in northern and central China compared to current conditions, and  $-4$  and  $-6^{\circ}\text{C}$  in southern areas (Zheng et al., 1998). Rainfall was between 400 and 600 mm lower in the regions under the current influence of the EAM (Zheng et al., 1998).

## 2.3 Simulated climate and $p_{\text{CO}_2}$

We used the model to analyse the  $\text{C}_3\text{-C}_4$  balance response to various conditions of  
20  $p_{\text{CO}_2}$  and climate. In order to deal with realistic distributions of climate parameters, climatic conditions were derived from the actual current climate observed in the two sites. Soil parameters were obtained from the FAO database. Cloudiness was kept  
25 constant in all simulations. We conducted two types of simulations with either constant  $p_{\text{CO}_2}$  or constant temperature and rainfall distributions.

First, current distributions of temperature and precipitation were modified to adjust

CPD

5, 1187–1213, 2009

### $\text{C}_3\text{-C}_4$ balance and $\delta^{13}\text{C}$ in simulated vegetation

O. Flores et al.

Title Page

Abstract

Introduction

Conclusions

References

Tables

Figures

◀

▶

◀

▶

Back

Close

Full Screen / Esc

Printer-friendly Version

Interactive Discussion



## C<sub>3</sub>-C<sub>4</sub> balance and δ<sup>13</sup>C in simulated vegetation

O. Flores et al.

[Title Page](#)
[Abstract](#)
[Introduction](#)
[Conclusions](#)
[References](#)
[Tables](#)
[Figures](#)
[Back](#)
[Close](#)
[Full Screen / Esc](#)
[Printer-friendly Version](#)
[Interactive Discussion](#)


the mean annual temperature ( $\bar{T}$ ) and annual rainfall ( $P_a$ ) to chosen values, while keeping the overall shape of the distributions. These simulations therefore reflect changes in annual values, not seasonality although the amplitude of the distribution changed. For a given change in temperature,  $\Delta\bar{T}$ , monthly means were adjusted as  $T'_i = T_i + \Delta T$ , where  $T_i$  is the mean temperature of month  $i$ . Monthly rainfall were modified in a similar way. For a given change in precipitation,  $\Delta P_a$ , monthly means were adjusted as  $P'_i = (1 + \frac{\Delta P_a}{P_a}) P_i$ , where  $P_i$  is the amount of precipitation of month  $i$  and  $P_a$  is the annual amount of precipitation. We ran the model at two different values of  $p_{\text{CO}_2}$ :

1. the LGM level (180 ppmv, Monnin et al., 2001),
2. the current level CO<sub>2</sub> (360 ppmv).

Second, we studied the influence of  $p_{\text{CO}_2}$  under fixed climatic conditions. Responses to  $p_{\text{CO}_2}$  were simulated in each site under the current climatic conditions and under estimated conditions at the LGM as described in the previous section.  $p_{\text{CO}_2}$  was changed gradually from 180 to 540 ppmv.

### 2.4 Model description

The BIOME4 model (Kaplan et al., 2002) is a process-based equilibrium model for terrestrial vegetation of the BIOME family (Prentice et al., 1992; Haxeltine and Prentice, 1996). The inputs fed in the model are monthly temperatures, rainfalls and cloudiness, absolute minimal temperatures, soil textures, latitude, atmospheric pressure through altitude and  $p_{\text{CO}_2}$ . Incoming solar radiation is calculated using current orbital parameters and average albedo. The model uses a two-layers description of soil, with different textures and depths. Run-off is evaluated, but lateral fluxes are not redistributed. Routines are included to approximate additional risks due to canopy fire and snow.

The models simulates 13 Plant Functional Types (PFT, Table 1). These PFTs are primarily constrained by absolute bioclimatic tolerance limits, such as the minimal sup-

## C<sub>3</sub>-C<sub>4</sub> balance and δ<sup>13</sup>C in simulated vegetation

O. Flores et al.

Title Page

Abstract

Introduction

Conclusions

References

Tables

Figures

⏪

⏩

◀

▶

Back

Close

Full Screen / Esc

Printer-friendly Version

Interactive Discussion



ported number of growing days over 5°C. These constraints determine whether the NPP of a given PFT is calculated or not. A photosynthesis-based growth procedure then optimizes the NPP and the optimal Leaf Area Index (LAI) for each of the potentially present PFTs under local climatic conditions. This calculation is based on a coupling between water and carbon fluxes in the plant (Haxeltine et al., 1996). Ten PFTs out of 13 are exclusively C<sub>3</sub>, one is exclusively C<sub>4</sub>, and two may use either pathway (Table 1). Water fluxes in the model depend on water availability in local soil and evapo-transpiration of soil and plants. Plant evapo-transpiration is controlled by the stomatal conductance of the PFTs which integrates to canopy conductance. In turn, the stomatal conductance controls  $\frac{c_i}{c_a}$  and thus the concentration of CO<sub>2</sub> available for photosynthesis.

Revisions of BIOME4 by Hatté and Guiot (2005) mostly concerned three aspects of photosynthesis and carbon isotopic discrimination depending on PFTs' pathways (see Hatté and Guiot, 2005, for details). The model of carbon isotopic discrimination originally followed Lloyd and Farquhar (1994) and produced estimates of Δ<sub>A</sub> which is the total discrimination against <sup>13</sup>CO<sub>2</sub> during carbon assimilation, i.e. from the atmosphere to the photosynthetates. Hatté and Guiot (2005) first imposed a lower limit on the  $\frac{c_i}{c_a}$  ratio for C<sub>3</sub> PFTs to avoid situations of stomatal closure. Second, the revised version takes into account the photosynthetic pathway of all potentially present PFTs – not only of the dominant, and weights isotopic fractionation by NPP which allows to take the stored carbon into account. Both pathways are taken into account in PFTs that can be either C<sub>3</sub> or C<sub>4</sub>. Third, refined isotopic fractionation during photosynthesis is simulating by taking temperature influence into account.

We studied two response variables obtained from the model outputs in the different scenarii: the fraction of NPP that is produced by C<sub>4</sub> photosynthesis:  $r_{C_4} = \frac{\sum_{C_4} NPP}{\sum NPP}$  where the sum is on the three PFTs that are obligate or facultative C<sub>4</sub> in the numerator and on all PFTs in the denominator (Table 1), and the carbon isotopic ratio, δ<sup>13</sup>C, at the bulk vegetation level. δ<sup>13</sup>C was obtained from the simulated values of Δ<sub>A</sub> as  $\delta^{13}C = \frac{\delta_{atm} - \Delta_A}{1 + \Delta_A}$



where  $\delta_{\text{atm}}$  is the atmospheric value which was fixed at  $-8\%$ .

### 3 Results

#### Change in $r_{C_4}$ and $\delta^{13}C$ from the LGM to current conditions

The proportion of  $C_4$  NPP ( $r_{C_4}$ ) was 6% in the vegetation simulated at Kuruyange and 0% at Lingtai under mean LGM conditions (Table 2). Starting from mean LGM conditions, the change in  $r_{C_4}$  was positive at the two sites, and lower at Kuruyange (+14%) than Lingtai (+23%). However, the change in  $r_{C_4}$  was highly sensible to incertitude in climatic parameters at Kuruyange, and showed negative values down to  $-22\%$  at the upper bound of the climatic parameters. Starting from average LGM conditions,  $\delta^{13}C$  decreased by  $-3.2\%$  at Kuruyange and increased by  $+1.9\%$  at Lingtai (Table 2). The signs of the change were consistent over the complete range of climatic parameters at the two sites.

#### Response to climate at fixed $p_{CO_2}$

The proportion of  $C_4$  NPP ( $r_{C_4}$ ) and the carbon isotopic composition of the vegetation ( $\delta^{13}C$ ) showed overall the same responses to temperature and precipitation in the two sites (Fig. 2 and 3). Changes in rainfall had weak effects on  $r_{C_4}$  and  $\delta^{13}C$ . The response of  $\delta^{13}C$  to temperature was hardly linear in the two sites and less variable at Kuruyange than at Lingtai. At Kuruyange, the response was hardly dependent of rainfall, except in cases of large decrease in rainfall ( $\Delta P_a < -500$  mm, Fig. 2a and 2b). The surface response was rough and more contrasted in Lingtai and water limitation occurred below  $-300$  mm (Fig. 2b and 2d).

Positive temperature changes implied increasing  $r_{C_4}$ , but no  $C_4$  NPP was simulated in cases of strong negative changes in mean annual temperature, whatever the change in rainfall or  $p_{CO_2}$  (Fig. 2). The maximal simulated value of  $r_{C_4}$  was 45% at Kuruyange

Title Page

Abstract

Introduction

Conclusions

References

Tables

Figures

⏪

⏩

◀

▶

Back

Close

Full Screen / Esc

Printer-friendly Version

Interactive Discussion



[Title Page](#)
[Abstract](#)
[Introduction](#)
[Conclusions](#)
[References](#)
[Tables](#)
[Figures](#)
[⏪](#)
[⏩](#)
[◀](#)
[▶](#)
[Back](#)
[Close](#)
[Full Screen / Esc](#)
[Printer-friendly Version](#)
[Interactive Discussion](#)


in the current condition of  $p_{\text{CO}_2}$  (Fig. 2a), and 61% in the LGM condition (Fig. 2c). These numbers were respectively 43% and 85% in Lingtai (Fig. 2b and 2d). The range of simulated  $\delta^{13}\text{C}$  was  $(-33, -23)\text{‰}$  at Kuruyange in the current condition of  $p_{\text{CO}_2}$  (Fig. 2a), and  $(-30, -18)\text{‰}$  in the LGM conditions (Fig. 2c). At Lingtai, these ranges were respectively  $(-35, -23)\text{‰}$  (Fig. 2b) and  $(-31, -19)$  (Fig. 2d).

## CO<sub>2</sub>- and temperature-induced change

In the following section, we focus on the responses of  $r_{\text{C}_4}$  and  $\delta^{13}\text{C}$  to  $p_{\text{CO}_2}$  and temperature. We investigate two different sets of climatic conditions:

1. the current climatic conditions of rainfall and temperature ( $\Delta\bar{T}=0$  and  $\Delta P_a=0$ , Fig. 1),
2. the average LGM conditions at Kuruyange:  $\Delta\bar{T}=-4^\circ\text{C}$ ,  $\Delta P_a=-350$  mm (Bonnetille et al., 1990; Bonnetille and Chalié, 2000), and at Lingtai:  $\Delta\bar{T}=-6^\circ\text{C}$ ,  $\Delta P_a=-400$  mm (Zheng et al., 1998).

The proportion of C<sub>4</sub> NPP ( $r_{\text{C}_4}$ ) and the carbon isotopic composition of the vegetation ( $\delta^{13}\text{C}$ ) both responded negatively to increase in  $p_{\text{CO}_2}$  (Fig. 4a and 4b). The two sites showed low simulated values of  $r_{\text{C}_4}$  in the climatic conditions of the LGM, whatever the  $p_{\text{CO}_2}$ . At Kuruyange, the simulated responses of  $\delta^{13}\text{C}$  were similar in the two sets of climatic conditions (Fig. 4a). On the contrary, transition from the LGM climate to the current climate at Lingtai induced an increase in  $\delta^{13}\text{C}$  (Fig. 4) whatever the  $p_{\text{CO}_2}$  (Fig. 4b).

The change in  $\delta^{13}\text{C}$  from the mean LGM to the current conditions can be decomposed in one variation due to climate and one to  $p_{\text{CO}_2}$ . Quantitatively,  $\delta^{13}\text{C}$  decreased by  $-3.2\text{‰}$  in Kuruyange (Table 2). The variation due to an increase in  $p_{\text{CO}_2}$  under constant climate was between  $-3.5$  (current conditions) and  $-4.6\text{‰}$  (LGM conditions), whereas the change due to the transition from the LGM to the current climate only was

between +0.3 (at current  $p_{\text{CO}_2}$ ) and +1.4‰ (at LGM  $p_{\text{CO}_2}$ ). In Lingtaï,  $\delta^{13}\text{C}$  increased by +1.9‰ (Table 2). Climate and  $p_{\text{CO}_2}$  interacted less than in Kuruyange, so that the change due to increasing  $p_{\text{CO}_2}$  was -4.1‰, and the change due to the transition in climatic conditions was +6.7‰ (Fig. 4b).

Positive temperature change increased in  $r_{\text{C}_4}$  and  $\delta^{13}\text{C}$  in all simulations (Fig. 4c and 4d). The increase was steeper in  $r_{\text{C}_4}$  in Kuruyange compared to Lingtaï. As seen in Fig. 2, no  $\text{C}_4$  photosynthesis occurred below  $-5^\circ\text{C}$  of temperature change at Kuruyange in both sets of tested conditions (Fig. 4c). At Lingtaï, the threshold on  $r_{\text{C}_4}$  was lower ( $\approx -7^\circ\text{C}$ , Fig. 4d).

## Response of the PFTs

We studied in detail the contribution of the different PFTs to the response profile of  $r_{\text{C}_4}$  and  $\delta^{13}\text{C}$  to temperature. The response of the different PFTs to temperature (Fig. 5) reveal the effect of abrupt changes in the composition of the vegetation in PFTs on  $r_{\text{C}_4}$  and  $\delta^{13}\text{C}$ , as seen also on the Figs. 2 and 3.

In the current conditions, tree PFTs had the highest NPP (tet, tft, tee, cot, Fig. 5a) in Kuruyange, followed by the tropical grass type (tog) and the woody desert type (wde). Major changes in the composition in PFTs occurred at values of  $\Delta\bar{T}$  around  $-4$ ,  $-2$ , 2 and  $5^\circ\text{C}$ . The temperate and tropical grass types coexisted for  $\Delta\bar{T}$  values between  $-4$  and  $-2^\circ\text{C}$ . In Lingtaï, the simulated NPPs were dominated by the “temperate deciduous tree” type (ted, Fig. 5b), the “temperate grass type” (teg) and the “woody desert type”. Major changes occurred above  $1^\circ\text{C}$  where the “conifer tree” type became productive, below  $-2^\circ\text{C}$  where the “boreal tree” types (bet, bdt) replaced the “temperate deciduous tree” type.

Increased  $p_{\text{CO}_2}$  from the LGM to the current level had a fertilization effect on all PFTs (Fig. 5). This effect led to decreased  $r_{\text{C}_4}$  and increased  $\delta^{13}\text{C}$  (Fig. 5).

Title Page

Abstract

Introduction

Conclusions

References

Tables

Figures

◀

▶

◀

▶

Back

Close

Full Screen / Esc

Printer-friendly Version

Interactive Discussion



## 4 Discussion

This study demonstrated interacting effects of climate and  $p_{\text{CO}_2}$  on the balance between  $\text{C}_3$  and  $\text{C}_4$  plants, and on the resulting  $\delta^{13}\text{C}$  signal in vegetation using simulation. Our study evidenced that climate had a prevailing effect over  $\text{CO}_2$  on the  $\text{C}_3$ - $\text{C}_4$  balance. Temperature was the most limiting factor on  $\text{C}_4$  NPP at the two studied sites, while the influence of rainfall was lower and differed across the sites. These results agree with studies of palaeosequences in central China (Gu et al., 2003; Zhang et al., 2003; Liu et al., 2005a) and in central America (Huang et al., 2001). Our results also show that changes in  $p_{\text{CO}_2}$  affected the  $\text{C}_3$ - $\text{C}_4$  balance, although more weakly, and implied changes in the vegetation  $\delta^{13}\text{C}$  signal. In another simulation study Jolly and Haxeltine (1997) concluded that change in  $p_{\text{CO}_2}$  level alone could drive large vegetation changes.

The overall responses of the  $\text{C}_3$ - $\text{C}_4$  balance to simulated climatic conditions were the same between the two sites, but the changes simulated in response to the transition from the LGM to the current conditions highly differed. Namely, the simulated balance at Kuruyange was between +20% and -22%, thus showing high sensitivity to the incertitude in climatic parameters. Palaeodata indicate that the proportion of  $\text{C}_4$  plants was higher at the LGM than in more recent records (Jolly et al., 1997; Aucour et al., 1999). Our results thus suggest that the anomaly in mean temperature at the LGM was probably closer to the estimated upper bound ( $\Delta\bar{T} = -2^\circ\text{C}$ , Bonnefille et al., 1990) than to the lower ( $\Delta\bar{T} = -6^\circ\text{C}$ ). At Lingtai, the proportion of  $\text{C}_4$  plants increased from the LGM to the current conditions, despite incertitude in climatic parameters, which corresponded to observations in core sequences (Gu et al., 2003; Wang et al., 2008).

The climatic conditions impacted  $\delta^{13}\text{C}$  differently across the two sites as a result of a double control of climate on the vegetation  $\delta^{13}\text{C}$ . First, a change from LGM climatic conditions to the current ones favored a higher proportion of  $\text{C}_4$  plants. The change in the  $\text{C}_3$ - $\text{C}_4$  balance induced an increase in the bulk  $\delta^{13}\text{C}$  which could be compensated

### $\text{C}_3$ - $\text{C}_4$ balance and $\delta^{13}\text{C}$ in simulated vegetation

O. Flores et al.

Title Page

Abstract

Introduction

Conclusions

References

Tables

Figures

⏪

⏩

◀

▶

Back

Close

Full Screen / Esc

Printer-friendly Version

Interactive Discussion



**C<sub>3</sub>-C<sub>4</sub> balance and  
 $\delta^{13}\text{C}$  in simulated  
vegetation**

O. Flores et al.

[Title Page](#)[Abstract](#)[Introduction](#)[Conclusions](#)[References](#)[Tables](#)[Figures](#)[⏪](#)[⏩](#)[◀](#)[▶](#)[Back](#)[Close](#)[Full Screen / Esc](#)[Printer-friendly Version](#)[Interactive Discussion](#)

by changes in the  $\delta^{13}\text{C}$  values of the C<sub>3</sub> pole (Boom et al., 2002; Wang et al., 2008), and of the C<sub>4</sub> pole to a lesser extent. This second effect was stronger in Lingtaï than in Kuruyange. In Kuruyange,  $p_{\text{CO}_2}$  had stronger influence on  $\delta^{13}\text{C}$  than in Lingtaï. The relative influence of climate and  $p_{\text{CO}_2}$  at the two sites relates to the current distribution of temperature and rainfall, the seasonality of which was conserved in the simulations. In Kuruyange, climatic conditions are less stressful than in Lingtaï where winter temperatures and rainfall are low. The effect of changing the mean annual temperature and total rainfall therefore induced a stronger response in  $\delta^{13}\text{C}$  at the chinese site compared to the african site.

The decrease of  $\delta^{13}\text{C}$  at Kuruyange and increase at Lingtaï during the transition from the LGM to the current conditions were in agreement with changes observed in cores from Kuryange (Aucour et al., 1999) and Lingtaï (Gu et al., 2003). The simulated change was lower in absolute value than the observed change at the two sites. Our purpose here was not to reconstruct the  $\delta^{13}\text{C}$  signal obtained in cores but to identify trends and effects of climate and  $p_{\text{CO}_2}$ . We used a process-based model that simulates the isotopic discrimination in the living vegetation (Kaplan et al., 2002). Adjustments to the model output need to be taken into account if one wants to approach values recorded in cores (Wang et al., 2008). The total organic content (TOC) of cores yields larger  $\delta^{13}\text{C}$  values than the  $^{13}\text{C}$  signal in the vegetation (Liu et al., 2005a) which is better estimated using *n*-alkanes (Boom et al., 2002; Wang et al., 2008). Here the model simulated the  $\delta^{13}\text{C}$  signal of the vegetation which is thus closer to that measured in *n*-alkanes.

The influence of climate and  $p_{\text{CO}_2}$  on the  $\delta^{13}\text{C}$  value of C<sub>3</sub>, and C<sub>4</sub> plants to a lesser extent highlights the need for controlling this effect when reconstructing the C<sub>3</sub>-C<sub>4</sub> balance. The drier conditions at the LGM induce a trend to higher  $\delta^{13}\text{C}$  in C<sub>3</sub> plants, as found currently along rainfall gradients (Liu et al., 2005b; Wang et al., 2008). Meanwhile, a lower  $p_{\text{CO}_2}$  also implies a higher  $\delta^{13}\text{C}$  (Lloyd and Farquhar, 1994). These effects add to the bioclimatic constraints limiting the potentially present PFTs with potential direct effects on the proportion of C<sub>4</sub> plants. Also pedogenesis effects increase

the  $\delta^{13}\text{C}$  of the soil organic matter with depth (Wang et al., 2008), whereas on a longer time scale, diagenesis depletes the organic matter in  $^{13}\text{C}$  to a small extent (Meyers, 1994). These effects thus enforce the need for correcting the  $\delta^{13}\text{C}$  of the  $\text{C}_3$  and  $\text{C}_4$  poles when reconstructing the  $\text{C}_3$ - $\text{C}_4$  balance (Wang et al., 2008).

The balance turns to the advantage of  $\text{C}_3$  plants at high temperature and rainfall when  $p_{\text{CO}_2}$  increases. For the  $\text{C}_4$  PFTs, the simulated catalytic activity of RuBisCO is independent of the ambient  $\text{CO}_2$  concentration (Haxeltine et al., 1996).  $\text{CO}_2$  interferes only with the Light Use Efficiency to reduce photosynthesis rates at low intercellular concentrations. On another hand, both effects are accounted in the computation of  $\text{C}_3$  photosynthesis rates. With increasing concentration of  $\text{CO}_2$ , these effects are reduced and  $\text{C}_3$  PFTs become more competitive. The domain of living conditions is reduced for  $\text{C}_4$  plants.

The analysis of the PFTs response showed that changes in their composition corresponded to important changes in the  $r_{\text{C}_4}$  response to temperature. The selection of potential PFTs in the model is essentially based on temperature constraints (mean temperature of the coldest month; absolute minimal temperature, number of days over 0 or 5°C) and snow cover. Hence, the list of present PFTs changes with temperature, as shown in Table 1. Local productivity peaks are linked with differential productivities of the PFTs, and to a succession of different PFTs in the domain of simulation. The study of present PFTs is then essential for a given site.

The competitiveness of  $\text{C}_4$  versus  $\text{C}_3$  plants improved in conditions of water stress, as indicated by large percentages of  $\text{C}_4$  NPP. Two effects can be called upon:  $\text{C}_4$  PFTs may be supported by their lower canopy conductance and/or lower evapotranspiration rates (Haxeltine et al., 1996). At low atmospheric  $\text{CO}_2$  levels, the simulated surfaces reveal the high sensitivity of  $\text{C}_4$  PFTs to climate. The evolution of the different PFTs shows that the observed excursions were due to strong variations in the NPP values of the present PFTs. In the model formulation, evapotranspiration depends on the canopy conductance, which is inversely proportional to the diffusion gradient of  $\text{CO}_2$  between the atmosphere and the intercellular air (Haxeltine and Prentice, 1996). Therefore,

## $\text{C}_3$ - $\text{C}_4$ balance and $\delta^{13}\text{C}$ in simulated vegetation

O. Flores et al.

Title Page

Abstract

Introduction

Conclusions

References

Tables

Figures

⏪

⏩

◀

▶

Back

Close

Full Screen / Esc

Printer-friendly Version

Interactive Discussion



increased  $p_{\text{CO}_2}$  tends to reduce evapotranspiration. Consequently, the PFTs are more tolerant to low annual rainfall.

## 5 Conclusions

Biome models based on physiological processes allow us to disentangle the impact of the climate and  $\text{CO}_2$  on ecosystems known to have been very sensitive in the past. Among these constraints, the atmospheric  $\text{CO}_2$  is strongly implied in the fundamental process of photosynthesis. Therefore, it seems that a biogeographical approach of the vegetation is insufficient to describe its evolution. Nowadays,  $\text{C}_4$  plants are rather known to be located at low altitude, under warm climatic conditions, in sub-desert or even desert areas, whereas  $\text{C}_3$  plants are found at higher altitude, under cooler conditions. The  $\text{C}_3$ - $\text{C}_4$  balance seems to fit an intuitive altitudinal or thermic gradient. In the present study,  $p_{\text{CO}_2}$ , as well as the climate, have important effects on this balance. Vegetation modelling is necessary to apprehend the evolution of the vegetation, since it allows a mechanistic approach taking account of natural processes.

Vegetation modelling can contribute to simulate the coexistence of various  $\text{C}_3$  and  $\text{C}_4$  poles. Then, a new contribution of vegetation modelling could be the estimation of  $\delta^{13}\text{C}$  for peculiar PFTs. This could provide a better reconstruction of the  $\text{C}_3$ - $\text{C}_4$  balance and allow comparisons between data and modelling results .

*Acknowledgements.* This paper is a contribution to the INCO-EU project (INCO-DC DG XII, ERB3514PL972473). We wish to thank Joël Guiot for kindly providing us the code of the revised version of BIOME4, and Adeline Fayolle for her constructive comments.

## References

Aucour, A. and Hillaire-Marcel, C.: Late Quaternary biomass changes from  $^{13}\text{C}$  measurements in a highland peatbog from equatorial Africa (Burundi), *Quaternary Res.*, 41, 225–233, 1994. 1189

### $\text{C}_3$ - $\text{C}_4$ balance and $\delta^{13}\text{C}$ in simulated vegetation

O. Flores et al.

Title Page

Abstract

Introduction

Conclusions

References

Tables

Figures

⏪

⏩

◀

▶

Back

Close

Full Screen / Esc

Printer-friendly Version

Interactive Discussion



**C<sub>3</sub>-C<sub>4</sub> balance and  
δ<sup>13</sup>C in simulated  
vegetation**

O. Flores et al.

Title Page

Abstract

Introduction

Conclusions

References

Tables

Figures

◀

▶

◀

▶

Back

Close

Full Screen / Esc

Printer-friendly Version

Interactive Discussion



Aucour, A., Bonnefille, R., and Hillaire-Marcel, C.: Sources and accumulation rates of organic carbon in an equatorial peatbog (Burundi, East Africa) during the Holocene: carbon isotope constraints, *Palaeogeogr. Palaeoclimatol.*, 150, 179–189, 1999. 1189, 1198, 1199

Balsam, W., Ji, J., and Chen, J.: Climatic interpretation of the Luochuan and Lingtaï loess sections, China, based on changing iron oxide mineralogy and magnetic susceptibility, *Earth Planet. Sci. Lett.*, 223, 335–348, doi:10.1016/j.epsl.2004.04.023, online available at: <http://www.sciencedirect.com/science/article/B6V61-4CMHW4H-1/2/f0b75eda3057d9e7caf9cb6e3559d74c>, 2004. 1192

Bonnefille, R. and Chalié, F.: Pollen-inferred precipitation time-series from equatorial mountains, Africa, the last 40 kyr BP, *Global Planet. Change*, 26, 25–50, doi:10.1016/S0921-8181(00)00032-1, online available at: <http://www.sciencedirect.com/science/article/B6VFO-41NK8KV-4/2/b9e6b181bc5605dabde493f8d445dd47>, 2000. 1192, 1196

Bonnefille, R. and Riollet, G.: The Kashiru pollen sequence (Burundi). *Palaeoclimatic implications for the last 40000 yr BP in tropical Africa*, *Quaternary Res.*, 30, 19–35, 1988. 1191

Bonnefille, R., Roeland, J. C., and Guiot, J.: Temperature and rainfall estimates for the past 40,000 years in equatorial Africa, *Nature*, 346, 347–349, doi:10.1038/346347a0, online available at: <http://dx.doi.org/10.1038/346347a0>, 1990. 1192, 1196, 1198

Bonnefille, R., Riollet, G., and Buchet, G.: Nouvelle séquence pollinique d'une tourbière de la crête Zaire-Nil (Burundi), *Rev. Palaeobot. palyno.*, 67, 315–330, 1991. 1191

Bonnefille, R., Riollet, G., Buchet, G., Icole, M., Lafont, R., Arnold, M., and Jolly, D.: Glacial/interglacial record from intertropical Africa, high resolution pollen and carbon data at Rusaka, Burundi, *Quaternary Sci. Rev.*, 14, 917–936, doi:10.1016/0277-3791(95)00071-2, online available at: <http://www.sciencedirect.com/science/article/B6VBC-3Y45T0F-G/2/935d72141738130a956b4197008cc7e9>, 1995. 1191

Boom, A., Marchant, R., Hooghiemstra, H., and Damst, J. S. S.: CO<sub>2</sub>- and temperature-controlled altitudinal shifts of C<sub>4</sub>- and C<sub>3</sub>-dominated grasslands allow reconstruction of palaeoatmospheric pCO<sub>2</sub>, *Palaeogeogr. Palaeoclimatol.*, 177, 151–168, doi:10.1016/S0031-0182(01)00357-1, online available at: <http://www.sciencedirect.com/science/article/B6V6R-44HWS2G-5/2/de7e43d6ba4f0823157de9e10feaed84>, 2002. 1199

Coetzee, J.: Pollen analytical studies in east and southern Africa, *Palaeoecol. Afr.*, 3, 1–146, 1967. 1191

Cole, D. R. and Monger, H. C.: Influence of atmospheric CO<sub>2</sub> on the decline of C<sub>4</sub> plants during the last deglaciation, *Nature*, 368, 533–536, doi:10.1038/368533a0, online available



at: <http://dx.doi.org/10.1038/368533a0>, 1994. 1189

Deines, P.: The isotopic composition of reduced inorganic carbon, in: Handbook of Environmental Isotope Chemistry: the terrestrial environment, edited by: Fritz, P. and Fontes, J., vol. 1, 329–406, Elsevier, Amsterdam, The Netherlands, 1980. 1190

5 Gu, Z. Y., Liu, Q., Xu, B., Han, J. M., Yang, S. L., Ding, Z. L., and Liu, T. S.: Climate as the dominant control on C-3 and C-4 plant abundance in the Loess Plateau: Organic carbon isotope evidence from the last glacial-interglacial loess-soil sequences, Chinese Sci. Bull., 48, 1271–1276, 2003. 1189, 1190, 1191, 1198, 1199

10 Guiot, J.: Statistical analyses of biospherical variability, in: Long-Term Climatic Variations: Data and Modelling, edited by: Duplessy, J. and Spyridakis, M., vol. 22 of NATO ASI Series I, 299–334, Springer-Verlag, New-York, USA, 1994. 1189

Guiot, J., Torre, F., Jolly, D., Peyron, O., Boreux, J. J., and Cheddadi, R.: Inverse vegetation modeling by Monte Carlo sampling to reconstruct palaeoclimates under changed precipitation seasonality and CO<sub>2</sub> conditions: application to glacial climate in Mediterranean region, Ecol. Modell., 127, 119–140, doi:10.1016/S0304-3800(99)00219-7, online available at: <http://www.sciencedirect.com/science/article/B6VBS-3YRVDGH-2/2/d93a6c4f34f7fa03462b434dfe4fd213>, 2000. 1189

Hamilton, A.: The interpretation of pollen diagrams from highland Uganda, Palaeoecol. Afr., 7, 45–149, 1972. 1191

20 Hamilton, A.: Environmental history of East Africa: a study of the Quaternary, Academic press, New York, USA, 328 pp., 1982. 1191

Hatté, C. and Guiot, J.: Palaeoprecipitation reconstruction by inverse modelling using the isotopic signal of loess organic matter: application to the Nußloch loess sequence (Rhine Valley, Germany), Clim. Dynam., 25, 315–327, doi:10.1007/s00382-005-0034-3, online available at: <http://dx.doi.org/10.1007/s00382-005-0034-3>, 2005. 1194

25 Haxeltine, A. and Prentice, I.: BIOME3: An equilibrium terrestrial biosphere model based on ecophysiological constraints, availability, and competition among plant functional types, Global Biogeochem. Cy., 10, 693–709, 1996. 1193, 1200

Haxeltine, A., Prentice, I., and Cresswell, I.: A coupled carbon and water flux model to predict vegetation structure, J. Veg. Sci., 7, 651–666, 1996. 1194, 1200, 1207

30 Huang, Y., Street-Perrott, F. A., Metcalfe, S. E., Brenner, M., Moreland, M., and Freeman, K. H.: Climate Change as the Dominant Control on Glacial-Interglacial Variations in C<sub>3</sub> and C<sub>4</sub> Plant Abundance, Science, 293, 1647–1651, doi:10.1126/science.1060143, online available

CPD

5, 1187–1213, 2009

## C<sub>3</sub>-C<sub>4</sub> balance and δ<sup>13</sup>C in simulated vegetation

O. Flores et al.

Title Page

Abstract

Introduction

Conclusions

References

Tables

Figures

◀

▶

◀

▶

Back

Close

Full Screen / Esc

Printer-friendly Version

Interactive Discussion



- at: <http://www.sciencemag.org/cgi/content/abstract/293/5535/1647>, 2001. 1189, 1190, 1198
- Jackson, R. B., Canadell, J., Ehleringer, J. R., Mooney, H. A., Sala, O. E., and Schulze, E. D.: A global analysis of root distributions for terrestrial biomes *Oecologia*, 108, 389–411, 1996.
- Jolly, D. and Haxeltine, A.: Effect of low glacial atmospheric CO<sub>2</sub> on tropical African montane vegetation, *Science*, 276, 786–788, online available at: <http://www.sciencemag.org/cgi/content/abstract/276/5313/786>, 1997. 1189, 1191, 1198
- Jolly, D., Bonnefille, R., and Roux, M.: Numerical interpretation of a high resolution Holocene pollen record from Burundi, *Palaeogeogr. Palaeoclimatol.*, 109, 357–370, 1994. 1191
- Jolly, D., Taylor, D., Marchant, R., Hamilton, A., Bonnefille, R., Buchet, G., and Riollet, G.: Vegetation dynamics in central Africa since 18000 yr BP: pollen records from the interlacustrine highlands of Burundi, Rwanda and western Uganda, *J. Biogeogr.*, 24, 495–512, online available at: <http://www3.interscience.wiley.com.gate1.inist.fr/journal/119154764/abstract>, 1997. 1189, 1191, 1198
- Kaplan, J. O., Prentice, I. C., and Buchmann, N.: The stable carbon isotope composition of the terrestrial biosphere: Modeling at scales from the leaf to the globe, *Global Biogeochem. Cy.*, 16, 1–11, doi:10.1029/2001GB001403, 2002. 1193, 1199
- Liu, W., Huang, Y., An, Z., Clemens, S. C., Li, L., Prell, W. L., and Ning, Y.: Summer monsoon intensity controls C<sub>4</sub>/C<sub>3</sub> plant abundance during the last 35 ka in the Chinese Loess Plateau: Carbon isotope evidence from bulk organic matter and individual leaf waxes, *Palaeogeogr. Palaeoclimatol.*, 220, 243–254, doi:10.1016/j.palaeo.2005.01.001, online available at: <http://www.sciencedirect.com.gate1.inist.fr/science/article/B6V6R-4FPX303-2/2/7e137eeb5316e97855f61d0cfbc23b10>, 2005a. 1189, 1190, 1198, 1199
- Liu, W., Xiahong, F., Youfeng, N., Qingle, Z., Yunning, C., and Zhisheng, A. N.: <sup>13</sup>C variation of C<sub>3</sub> and C<sub>4</sub> plants across an Asian monsoon rainfall gradient in arid northwestern China, *Glob. Change Biol.*, 11, 1094–1100, doi:10.1111/j.1365-2486.2005.00969.x, online available at: <http://dx.doi.org/10.1111/j.1365-2486.2005.00969.x>, 2005b. 1190, 1199
- Lloyd, J. and Farquhar, G. D.: <sup>13</sup>C discrimination during CO<sub>2</sub> assimilation by the terrestrial biosphere, *Oecol.*, 99, 201–215, doi:{10.1007/BF00627732}, online available at: <http://dx.doi.org/10.1007/BF00627732>, 1994. 1194, 1199
- Meyers, P. A.: Preservation of elemental and isotopic source identification of sedimentary organic matter, *Chem. Geol.*, 114, 289–302, doi:10.1016/0009-2541(94)90059-0, online available at: <http://www.sciencedirect.com/science/article/B6V5Y-488G61V-97/2/1d2f736e88f649cb9896848d6a51d6da>, 1994. 1200

CPD

5, 1187–1213, 2009

## C<sub>3</sub>-C<sub>4</sub> balance and δ<sup>13</sup>C in simulated vegetation

O. Flores et al.

Title Page

Abstract

Introduction

Conclusions

References

Tables

Figures

◀

▶

◀

▶

Back

Close

Full Screen / Esc

Printer-friendly Version

Interactive Discussion



**C<sub>3</sub>-C<sub>4</sub> balance and  
δ<sup>13</sup>C in simulated  
vegetation**

O. Flores et al.

Title Page

Abstract

Introduction

Conclusions

References

Tables

Figures

◀

▶

◀

▶

Back

Close

Full Screen / Esc

Printer-friendly Version

Interactive Discussion



- Monnin, E., Indermuhle, A., Dallenbach, A., Fluckiger, J., Stauffer, B., Stocker, T. F., Raynaud, D., and Barnola, J.-M.: Atmospheric CO<sub>2</sub> Concentrations over the Last Glacial Termination, *Science*, 291, 112–114, doi:10.1126/science.291.5501.112, online available at: <http://www.sciencemag.org/cgi/content/abstract/291/5501/112>, 2001. 1193
- 5 New, M., Lister, D., Hulme, M., and Makin, I.: A high-resolution data set of surface climate over global land areas, *Climate Res.*, 21, 1–25, 2002. 1192, 1209
- Prentice, I. C., Cramer, W., Harrison, S. P., Leemans, R., Monserud, R. A., and Solomon, A. M.: A global biome model based on plant physiology and dominance, soil properties and climate, *J. Biogeogr.*, 19, 117–134, 1992. 1193
- 10 Sage, R. F.: The evolution of C<sub>4</sub> photosynthesis, *New Phytol.*, 161, 341–370, doi:10.1111/j.1469-8137.2004.00974.x, online available at: <http://www.blackwell-synergy.com/doi/abs/10.1111/j.1469-8137.2004.00974.x>, 2004. 1189
- Schefusz, E., Schouten, S., Jansen, J. H. F., and Damste, J. S. S.: African vegetation controlled by tropical sea surface temperatures in the mid-Pleistocene period, *Nature*, 422, 418–421, doi:10.1038/nature01500, online available at: <http://dx.doi.org/10.1038/nature01500>, 2003. 1190
- 15 Street-Perrott, F. A., Huang, Y., Perrott, R. A., Eglinton, G., Barker, P., Khelifa, L. B., Harkness, D. D., and Olago, D. O.: Impact of Lower Atmospheric Carbon Dioxide on Tropical Mountain Ecosystems, *Science*, 278, 1422–1426, doi:10.1126/science.278.5342.1422, online available at: <http://www.sciencemag.org.gate1.inist.fr/cgi/content/abstract/278/5342/1422>, 1997. 1189
- 20 Taylor, D.: Late Quaternary pollen records from two Ugandan mires: evidence for environmental change in the Rukiga Highlands of southwest Uganda, *Palaeogeogr. Palaeoclimatol.*, 80, 283–300, 1990. 1191
- 25 Taylor, D.: Pollen evidence from Muchoya swamp, Rukiga Highlands (Uganda), for abrupt changes in vegetation during the last ca. 21000 years, *B. Soc. Geol. Fr.*, 163, 77–82, 1992. 1191
- Taylor, D.: Environmental change in montane southwest Uganda: a pollen record for the Holocene from Ahakagyezi swamp, *The Holocene*, 3, 324–332, 1993. 1191
- 30 Vincens, A.: Late Quaternary vegetation history of the South-Tanganyika Basin. Climatic implications in south central Africa, *Palaeogeogr. Palaeoclimatol.*, 86, 207–226, 1991. 1191
- Wand, S. J. E., Midgley, G. F., Jones, M. H., and Curtis, P. S.: Responses of wild C<sub>4</sub> and C<sub>3</sub> grass (Poaceae) species to elevated atmospheric CO<sub>2</sub> concentration: a meta-analytic

test of current theories and perceptions, *Global Change Biology*, 5, 723–741, doi:10.1046/j.1365-2486.1999.00265.x, online available at: <http://www3.interscience.wiley.com/journal/119098780/abstract>, 1999. 1189

Wang, G., Feng, X., Han, J., Zhou, L., Tan, W., and Su, F.: Paleovegetation reconstruction using  $\delta^{13}\text{C}$  of Soil Organic Matter, *Biogeosciences*, 5, 1325–1337, 2008, <http://www.biogeosciences.net/5/1325/2008/>. 1189, 1190, 1191, 1198, 1199, 1200

Ward, J. K., Tissue, D. T., Thomas, R. B., and Strain, B. R.: Comparative responses of model  $\text{C}_3$  and  $\text{C}_4$  plants to drought in low and elevated  $\text{CO}_2$ , *Glob. Change Biol.*, 5, 857–867, 1999. 1189

Yu, G., Chen, X., Ni, J., Cheddadi, R., Guiot, J., Han, H., Harrison, S. P., Huang, C., Ke, M., Kong, Z., Li, S., Li, W., Liew, P., Liu, G., Liu, J., Liu, Q., Liu, K., Prentice, I. C., Qui, W., Ren, G., Song, C., Sugita, S., Sun, X., Tang, L., Campo, E. V., Xia, Y., Xu, Q., Yan, S., Yang, X., Zhao, J., and Zheng, Z.: Palaeovegetation of China: a pollen data-based synthesis for the mid-Holocene and last glacial maximum, *J. Biogeogr.*, 27, 635–664, doi:10.1046/j.1365-2699.2000.00431.x, online available at: <http://dx.doi.org/10.1046/j.1365-2699.2000.00431.x>, 2000. 1191

Zhang, Z., Zhao, M., Lu, H., and Faiia, A. M.: Lower temperature as the main cause of  $\text{C}_4$  plant declines during the glacial periods on the Chinese Loess Plateau, *Earth Planet. Sci. Lett.*, 214, 467–481, doi:10.1016/S0012-821X(03)00387-X, online available at: <http://www.sciencedirect.com.gate1.inist.fr/science/article/B6V61-49CR9VN-3/2/5c68ec345fcd900c4a6afe8cfba8b157>, 2003. 1189, 1190, 1198

Zheng, Z., Baoyin, Y., and Petit-Maire, N.: Paleoenvironments in China during the Last Glacial Maximum and the Holocene optimum, *Episodes*, 21, 152–158, 1998. 1192, 1196

CPD

5, 1187–1213, 2009

## $\text{C}_3$ - $\text{C}_4$ balance and $\delta^{13}\text{C}$ in simulated vegetation

O. Flores et al.

Title Page

Abstract

Introduction

Conclusions

References

Tables

Figures

◀

▶

◀

▶

Back

Close

Full Screen / Esc

Printer-friendly Version

Interactive Discussion



## C<sub>3</sub>-C<sub>4</sub> balance and $\delta^{13}\text{C}$ in simulated vegetation

O. Flores et al.

**Table 1.** Characteristics of Plant Functional Types (PFT) in BIOME4 (Haxeltine et al., 1996). Phe.: phenology; *E*, evergreen; *S*, summergreen; *R*, raingreen;  $g_C$ : maximal value for minimum canopy conductance;  $E_{\max}$ : maximum value of supported daily transpiration rate; value of *sw* below which raingreen leaves drop; value of *sw* above which raingreen leaves appear;  $R_{\text{top}}$ : fraction of roots in top soil layer, 30 cm from Jackson et al. (1996); LL: expected leaf longevity in months; GDD5: annual growing degree-days (GDD) above base temperatures of 5 and 0°C required for full leaf out; P.P.: photosynthetic pathway, C<sub>3</sub>, C<sub>4</sub>, or both.

Label	Type	Phe.	$g_C$	$E_{\max}$		$R_{\text{top}}$	LL	GDD <sub>5</sub>	GDD <sub>0</sub>	P.P.
tet	Tropical evergreen tree	E	0.5	10		0.69	18			C <sub>3</sub>
tdt	Tropical drought-deciduous tree	R	0.5	10	0.5	0.6	0.70	9		C <sub>3</sub>
tee	Temperate broadleaved evergreen tree	E	0.2	4.8		0.67	18			C <sub>3</sub>
ted	Temperate deciduous tree	S	0.8	10		0.65	7	200		C <sub>3</sub>
cot	Cool conifer tree	E	0.2	4.8		0.52	30			C <sub>3</sub>
bet	Boreal evergreen tree	E	0.5	4.5		0.83	24			C <sub>3</sub>
bdt	Boreal deciduous tree	S	0.8	10		0.83	24	200		C <sub>3</sub>
teg	Temperate grass	R	0.8	6.5	0.2	0.3	0.83	8	100	C <sub>3</sub> /C <sub>4</sub>
trg	Tropical grass	R	0.8	8	0.2	0.3	0.57	10		C <sub>4</sub>
wde	Woody desert type	E	0.1	1		0.53	12			C <sub>3</sub> /C <sub>4</sub>
tsh	Tundra shrub	E	0.8	1		0.93	8			C <sub>3</sub>
che	Cold herbaceous type	S	0.8	1		0.93	8		25	C <sub>3</sub>
lfo	Lichen/forb	E	0.8	1		0.93	8			C <sub>3</sub>

Title Page

Abstract

Introduction

Conclusions

References

Tables

Figures

◀

▶

◀

▶

Back

Close

Full Screen / Esc

Printer-friendly Version

Interactive Discussion



## C<sub>3</sub>-C<sub>4</sub> balance and $\delta^{13}\text{C}$ in simulated vegetation

O. Flores et al.

**Table 2.** Simulated C<sub>3</sub>-C<sub>4</sub> balance ( $r_{\text{C}_4}$ , the proportion of C<sub>4</sub> Net Primary Production, NPP) and  $\delta^{13}\text{C}$  of the vegetation at Kuruyange (Burundi) and Lingtai (China) in the conditions of the Last Glacial Maximum (LGM:  $p_{\text{CO}_2}=180$  ppmv; Kuryange:  $\Delta\bar{T}=-4\pm 2^\circ\text{C}$ ,  $\Delta P_a=-450\pm 250$  mm; Lingtai:  $\Delta\bar{T}=8\pm 2^\circ\text{C}$ ,  $\Delta P_a=-500\pm 100$  mm) and in the current conditions ( $p_{\text{CO}_2}=360$  ppmv;  $\Delta\bar{T}=0^\circ\text{C}$ ,  $\Delta P_a=0$  mm). The numbers in the square brackets indicate the simulated values using the extreme values of the climatic parameters.

	Kuruyange		Lingtai	
	$r_{\text{C}_4}$ (%)	$\delta^{13}\text{C}$ (‰)	$r_{\text{C}_4}$ (%)	$\delta^{13}\text{C}$ (‰)
LGM	6 [0, 36]	-26.7 [-28.0, -23.4]	0 [0, 6]	-28.0 [-29.7, -27.4]
Current	20	-29.9	23	-26.1
$\Delta$	+14 [+20, -22]	-3.2 [-1.9, -6.5]	+23 [+23, +17]	+1.9 [+3.6, +1.3]

Title Page

Abstract

Introduction

Conclusions

References

Tables

Figures

◀

▶

◀

▶

Back

Close

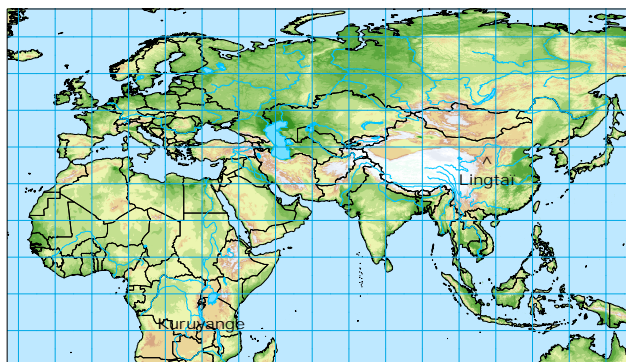
Full Screen / Esc

Printer-friendly Version

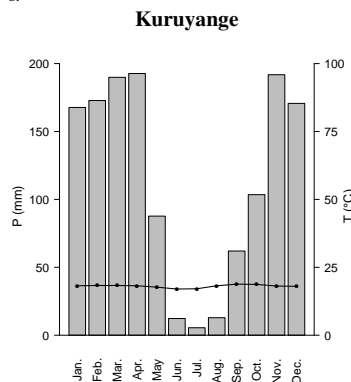
Interactive Discussion



a.



b.



c.

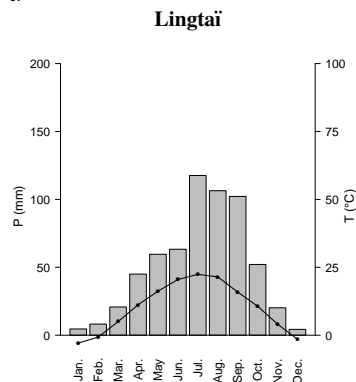


**Fig. 1.** (a) Location of the two study sites: Kuruyange in the intertropical highlands of Burundi, and Lingtai on the Loess Plateau in central China; (b) Climatic diagram of Kuruyange (Burundi, mean annual temperature,  $\bar{T}=18.1^{\circ}\text{C}$ , annual rainfall amount,  $P_{\text{ann}}=1380\text{ mm}$ ); (c) Climatic diagram of Lingtai (China, mean annual temperature,  $\bar{T}=10.2^{\circ}\text{C}$ , annual rainfall amount,  $P_{\text{ann}}=600\text{ mm}$ ), data taken from New et al. (2002).

Title Page

Abstract

Introduction

Conclusions

References

Tables

Figures

◀

▶

◀

▶

Back

Close

Full Screen / Esc

Printer-friendly Version

Interactive Discussion



## C<sub>3</sub>-C<sub>4</sub> balance and $\delta^{13}\text{C}$ in simulated vegetation

O. Flores et al.

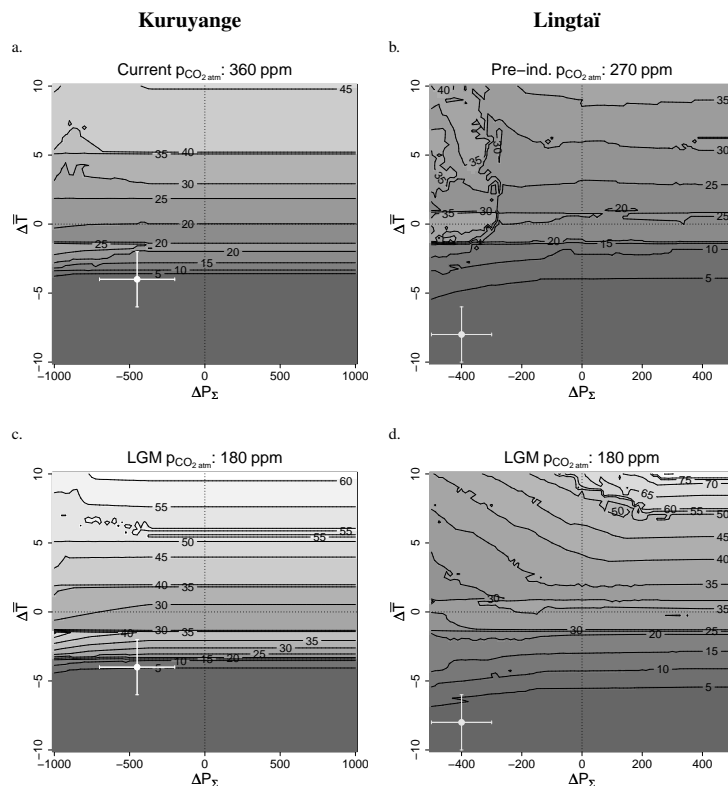


**Fig. 2.** Percentage of total NPP produced by C<sub>4</sub> photosynthetic as predicted by BIOME4 at Kuruyange (Burundi, **a** and **c**) and Lingtai (China, **b** and **d**).  $\Delta\bar{T}$ ,  $\Delta P_a$  represent the simulated changes in mean annual temperature and annual rainfall with regards to the current values. Two cases of  $p_{\text{CO}_2}$  are presented: current level (360 ppm in **a** and **c**), and Last Glacial Maximum level (LGM, 180 ppm in **b** and **d**). Dashed lines indicates the current climatic conditions ( $\Delta\bar{T}=0$ ,  $\Delta P_a=0$ ). The asterisk corresponds to climatic parameters during the LGM.

Title Page

Abstract

Introduction

Conclusions

References

Tables

Figures

◀

▶

◀

▶

Back

Close

Full Screen / Esc

Printer-friendly Version

Interactive Discussion





## $C_3$ - $C_4$ balance and $\delta^{13}C$ in simulated vegetation

O. Flores et al.

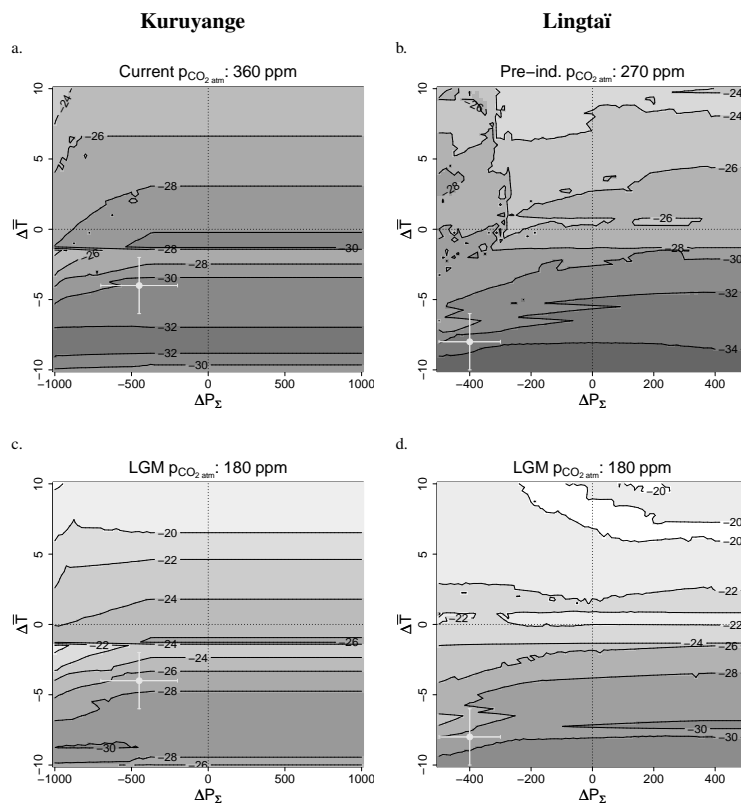


**Fig. 3.** Carbon isotope fractionation in predicted vegetation at Kuruyange (Burundi, **a** and **c**) and Lingtai (China, **b** and **d**).  $\Delta\bar{T}$ ,  $\Delta P_a$  represent the simulated changes in mean annual temperature and annual rainfall. Two cases of  $p_{CO_2}$  are presented: current level (360 ppm in **a** and **c**), and Last Glacial Maximum level (LGM, 180 ppm in **b** and **d**). Dashed lines indicate the current climatic conditions ( $\Delta\bar{T}=0$ ,  $\Delta P_a=0$ ). The asterisk corresponds to climatic parameters during the LMG.

Title Page

Abstract

Introduction

Conclusions

References

Tables

Figures

◀

▶

◀

▶

Back

Close

Full Screen / Esc

Printer-friendly Version

Interactive Discussion



## C<sub>3</sub>-C<sub>4</sub> balance and $\delta^{13}\text{C}$ in simulated vegetation

O. Flores et al.

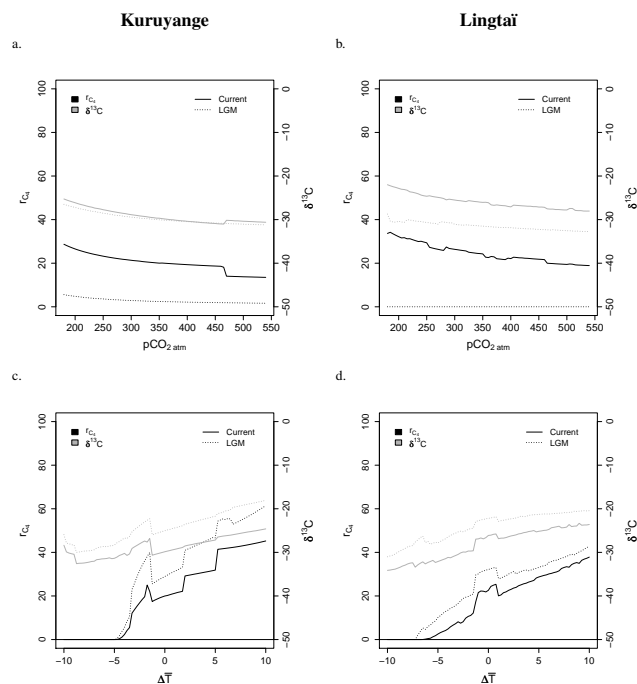


**Fig. 4.** Top: Response profile of the percentage of C<sub>4</sub> NPP ( $r_{C_4}$ , black lines) and carbon isotope fractionation ( $\delta^{13}\text{C}$ , gray lines) to  $p\text{CO}_2$  in the simulated vegetation at Kuruyange (Burundi, **a**) and Lingtai (China, **b**). Thick solid and dotted lines correspond respectively to the current climatic conditions at the site ( $\Delta\bar{T}=0$ ,  $\Delta P_a=0$ ) and the mean LGM climatic conditions. Bottom: Response profile of the percentage of C<sub>4</sub> NPP ( $r_{C_4}$ , black lines) and carbon isotope fractionation ( $\delta^{13}\text{C}$ , gray lines) to temperature in the simulated vegetation at Kuruyange (**c**) and Lingtai (**d**).  $\Delta\bar{T}$  represents the simulated change in mean annual temperature. Thick solid and dotted lines correspond to the current  $p\text{CO}_2$  and rainfall at the site and the mean LGM climatic conditions.

Title Page

Abstract

Introduction

Conclusions

References

Tables

Figures

◀

▶

◀

▶

Back

Close

Full Screen / Esc

Printer-friendly Version

Interactive Discussion



## C<sub>3</sub>-C<sub>4</sub> balance and $\delta^{13}\text{C}$ in simulated vegetation

O. Flores et al.

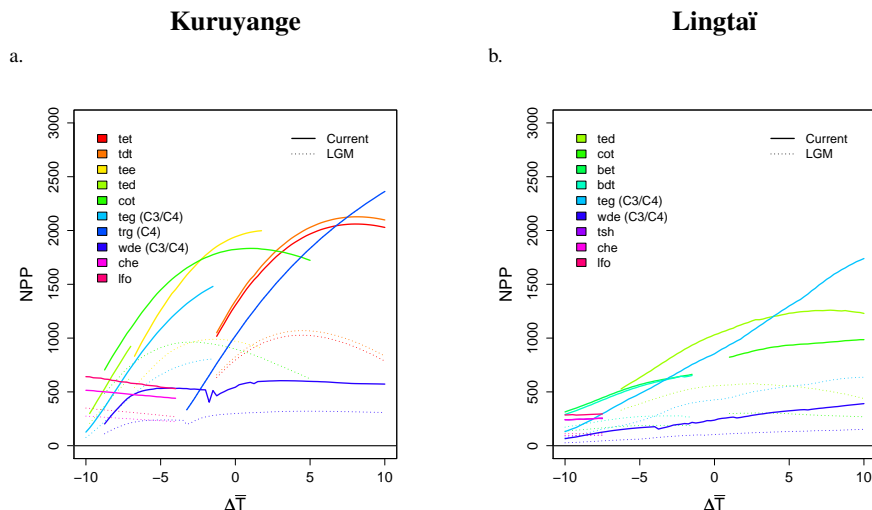


**Fig. 5.** NPP response profile to temperature of the simulated PFTs at Kuruyange (Burundi, **a**) and Lingtai (China, **b**). Thick solid and dotted lines correspond to the current  $p_{\text{CO}_2}$  and rainfall at the site and the mean LGM climatic conditions. The PFTs are labeled according to Table 1: tet, tropical evergreen tree; trt, tropical drought-deciduous tree; tbe, temperate broadleaved evergreen tree; tst, temperate deciduous tree; ctc, cool conifer tree; bec, boreal evergreen tree; bst, boreal deciduous tree; teg, temperate grass; tog, tropical grass; wde, woody desert type; tsh, tundra shrub; che, cold herbaceous type; lfo, lichen/forb.

[Title Page](#)
[Abstract](#)
[Introduction](#)
[Conclusions](#)
[References](#)
[Tables](#)
[Figures](#)
[Back](#)
[Close](#)
[Full Screen / Esc](#)
[Printer-friendly Version](#)
[Interactive Discussion](#)
